Nonisothermal Laminar Contracted Flow

Temperature and velocity profiles and pressure losses were computed for laminar, temperature-dependent Newtonian flow from a stream tube through an abrupt contraction into and through the entrance region of a smaller coaxial tube, in which the fluid was cooled or heated at constant wall temperature. The equations of motion and energy, including axial diffusion and viscous dissipation, were solved numerically for diameter ratios of one and two, a practical temperature range, and N_{Pe} and N_{Re} up to 100. Entrance temperatures and velocities are far from uniform, and pressure losses are greater than those computed using simplified equations and uniform entrance temperatures and velocities.

E. B. CHRISTIANSEN and S. J. KELSEY

Department of Chemical Engineering
The University of Utah
Salt Lake City, Utah 84112

SCOPE

The purpose of the presently reported study was to provide more accurate means for predicting pressure losses and the nature of the velocity and temperature fields at the entrance of and in the tubes of such equipment as shell-and-tube heat exchangers, chemical and nuclear reactors, and similar devices. Improved means for predicting such pressure losses and temperature and velocity fields should provide a basis for more effective and economical heat-exchanger design. Also, the nature of these temperature and velocity fields has an important influence on the progress of a chemical reaction and is important in the design and analysis of data from tubular chemical reactors.

Recent as well as earlier theoretical and experimental studies of flow in a tube accompanied by heat exchange with the tube walls have demonstrated that the dependence of viscosity on temperature can importantly affect pressure losses and heat transfer. In some recent numerical solutions of the equations of motion and energy in which the dependence of viscosity on temperature is accounted for, it was assumed that flow at the tube entrance is parabolic and that radial convection, inertial terms, axial diffusion, and viscous dissipation are negligible. Some improved numerical solutions account for temperature-dependent viscosity, radial flow, and inertial effects but are restricted to uniform tube-entrance velocities and temperatures. Although these solutions approximate some situations, it is known that entrance velocity profiles are not flat in laminar, isothermal flow, particularly in the flow geometry of concern here, and that axial diffusion and viscous dissipation may have important effects. The effects of temperature-dependent flow, combined with those of axial diffusion and viscous dissipation, for the case of interest here have not, to our knowledge, been clearly defined in previous reports.

In the presently reported study, flow from the header into the tubes of a shell-and-tube heat exchanger or reactor was approximated by flow from a larger stream tube (a stream tube has a frictionless wall) through an abrupt contraction into and through the flow- and temperature-development region of a smaller coaxial tube. The wall of the small tube was real (fluid adhered to it) and was at a higher or lower constant temperature than that of the entering fluid. The contracting surface connecting the tubes was real, flat, and perpendicular to the common tube axis.

The general equations of motion and energy, including axial-diffusion and viscous-dissipation terms, were solved numerically, by means of quasilinearization and the method of lines, for temperature-dependent laminar Newtonian flow through the just-described approximation. Computational costs and instabilities limited our computations largely to a tube-diameter ratio of two and to N_{Re} and N_{Pe} less than 100. However, a good range of ψ(H)—an index to the effects of the dependence of viscosity on temperature—was explored. The results in which viscous dissipation was taken into account were very restricted and are not included here.

CONCLUSIONS AND SIGNIFICANCE

The results are presented as plots of temperature and velocity profiles and pressure losses as functions of axial position $\psi(H)$, N_{Re}, and N_{Pe}.

Temperature and velocity fields are altered by diffusion at significant distances upstream of the entrance—over 2½ diameters at high $\psi(H)$ and low N_{Pe}. The entrance temperature profiles depend principally on N_{Pe} and, to a lesser extent, on $\psi(H)$ but are not uniform; and the gradient at the wall is always finite in contrast to results for cases in which axial diffusion has been neglected. Within the range of variables investigated, entrance velocities are far from uniform or parabolic, even for the case in which the diameter of the stream tube is the same as that of the real tube. At N_{Re} greater than about 30 to 50, concavities in the entrance velocity profiles—similar to those observed experimentally and computed for the case of isothermal flow—may be present. In some cases, computed centerline velocities are as much as 20% less than those nearer the wall. Other variables being constant, the depth of the concavity increases with N_{Re}, while depending principally on N_{Pe}, it is increased, decreased, or affected little by either cooling or heating.

The excess pressure loss attributable to flow develop-

ment when the diameter ratio is unity is significantly greater than that computed by use of the simplified equations. When the diameter ratio is two, the excess pressure loss includes the effect of flow contraction as well as that of flow development and is much greater than that computed by use of the simplifying assumptions.

Many solutions of boundary-layer equations, including some for non-Newtonian fluids (Chen et al., 1970; Collins and Schowalter, 1963; Michiyoshi et al., 1966), and some numerical solutions of simplified equations of motion (Christiansen and Lemmon, 1965; Hornbeck, 1965; Lemmon, 1963) have been reported for laminar, isothermal flow through a real-tube entrance region for which a flat entrance velocity and constant fluid properties were assumed (see Christiansen et al., 1972, and Christiansen and Lemmon, 1965, for comparisons of Newtonian flow results). More recently, numerical solutions of somewhat restricted equations of motion and energy (radial flow, inertial terms, axial diffusion, and viscous dissipation were neglected) for temperature-dependent Newtonian and non-Newtonian flow accompanied by heat transfer have been reported (Newtonian and power-law flow: Christiansen and Craig, 1962; Christiansen and Jensen, 1969; Christiansen et al., 1966; Jensen, 1963; Bingham flow: Jensen, 1963; Powell-Eyring flow: Christiansen and Jensen, 1962; Jensen, 1963) for the case where the fluid in fully developed flow in a real tube enters a region in which the tube wall is abruptly at a higher or lower constant temperature than that of the fluid. Of greater interest here are some numerical solutions of restricted equations of motion and energy in which axial diffusion of momentum and energy, viscous dissipation, and the radial component of the momentum equations are neglected for temperature-dependent developing flow and developing temperature field when the entering velocity and temperature profiles are uniform (Lemmon, 1963; Rosenberg and Hellums, 1965; Shinohara, 1972) and for a modification of these using boundary-layer theory near the entrance coupled with numerical solutions of the restricted transport equations for the remainder of the entrance region (McKillop et al., 1970).

However, most pertinent are the numerical solutions of the general equations of motion—including axial-diffusion, radial-convection, and inertial terms—by Wang and Longwell (1964) for laminar Newtonian flow between parallel plates, preceded by plates of the same spacing but with frictionless surfaces; by Vrentas, Duda, and Bargeron (1966) for Newtonian flow from a stream tube through the entrance region of a real tube of the same diameter; and by Christiansen and Carter (1969) and by Christiansen et al. (1972) for contracted Newtonian and power-law non-Newtonian flow for stream-tube/real-tube (ST-RT) and real-tube/real-tube (RT-RT) geometries and for values of β, the ratio of the diameter of the upstream tube to that of the downstream tube, varying from 1 to 8.

We present here results from an extension of our investigations (Christiansen and Carter, 1969; Christiansen et al., 1972) to nonisothermal temperature-dependent ST-RT and RT-RT contracted Newtonian flow. In these studies, there is heat exchange with the surface of the smaller tube, which is at a higher or lower constant temperature than the initial temperature of the fluid.

THEORETICAL APPROACH

The general equation of motion in dimensionless vorticity-transport-equation form—similar to that used by Vrentas et al. (1966), except that the viscosity μ is a variable included in f^*—follows:

$$\nabla^{*2}(\omega^* f^*) = \frac{1}{r^*}\left[\frac{\partial\psi^*}{\partial r^*}\frac{\partial\omega^*}{\partial z^*} - \frac{\partial\psi^*}{\partial z^*}\frac{\partial\omega^*}{\partial r^*}\right] + \omega^*\left[\frac{1}{r^{*2}}\frac{\partial\psi^*}{\partial z^*} + \frac{f^*}{r^{*2}}\right] + 2\omega^*\frac{\partial^2 f^*}{\partial z^{*2}} - \frac{2}{r^*}\frac{\partial^2 f^*}{\partial r^*\,\partial z^*}\left[2\frac{\partial^2\psi^*}{\partial r^*\,\partial z^*} - \frac{1}{r^*}\frac{\partial\psi^*}{\partial z^*}\right] - \frac{2}{r^*}\frac{\partial^2\psi}{\partial z^{*2}}\left[\frac{\partial^2 f^*}{\partial z^{*2}} - \frac{\partial^2 f^*}{\partial r^{*2}}\right], \quad (1)$$

where

$$\nabla^{*2} = \frac{1}{R^2}\left[\frac{\partial^2}{\partial r^{*2}} + \frac{1}{r^*}\frac{\partial}{\partial r^*} + \frac{\partial^2}{\partial z^{*2}}\right],$$

$$\omega^* = \frac{R\omega}{V_0},$$

$$f^* = \frac{f}{R\,V_0} = \frac{-\mu}{\rho\,R\,V_0},$$

$$r^* = \frac{r}{R},$$

$$\psi^* = \frac{\psi}{R^2\,V_0},$$

$$z^* = \frac{z}{R}.$$

Equation (1) and the vorticity-stream-function relationship,

$$\nabla^{*2}\psi^* = r^*\,\omega^* + \frac{2}{r^*}\frac{\partial\psi^*}{\partial r^*}, \quad (2)$$

constitute the general flow formulation.

The general energy equation, in terms of dimensionless variables, is

$$\nabla^{*2} T^* = \frac{N_{Pe}}{2}\frac{1}{r^*}\left[\frac{\partial\psi^*}{\partial z^*}\frac{\partial T^*}{\partial r^*} - \frac{\partial\psi^*}{\partial r^*}\frac{\partial T^*}{\partial z^*}\right] - N_{Brn}\frac{\mu}{\mu_0}\Phi_v^*, \quad (3)$$

where

$$T^* = \frac{T - T_{-\infty}}{T_w - T_{-\infty}},$$

$$N_{Pe} = \frac{\rho\,V_0\,D\,c_p}{k} = N_{Re}\,N_{Pr},$$

$$N_{Brn} = \frac{\mu_0}{\mu}\,N_{Br} = \frac{\mu_0\,V_0^2}{k(T_w - T_{-\infty})},$$

$$\Phi_v^* = \frac{R}{V_0^2}\Phi_v = \frac{4}{r^{*2}}\left[\frac{1}{r^{*2}}\left[\frac{\partial\psi^*}{\partial z^*}\right]^2 - \frac{1}{r^*}\frac{\partial\psi^*}{\partial z^*}\frac{\partial^2\psi^*}{\partial r^*\,\partial z^*} + \left[\frac{\partial^2\psi^*}{\partial r^*\,\partial z^*}\right]^2\right] + \left[\frac{2}{r^*}\frac{\partial^2\psi^*}{\partial z^{*2}} - \omega^*\right]^2.$$

The introduction of a reference viscosity μ_0 allows formulation of a nonshear-rate-dependent Brinkman number N_{Br_n}.

Equations (1) and (3) were coupled with the relationship

$$\tau = \mu_0 \dot{\gamma} e^{\Delta H^\dagger/RT} \quad (4)$$

where τ is the shear stress, $\dot{\gamma}$ is the shear rate, μ_0 is a constant, $\Delta H^\dagger$ is the flow activation energy, and R is the Boltzman constant per mole.

For Newtonian flow

$$f^* = -\frac{1}{N_{Re}} \exp\left[\psi(H)\frac{1-T^*}{1+\dfrac{(1-T')T^*}{T'}}\right][1+\exp[-\psi(H)]], \quad (5)$$

where N_{Re} is an average of the smaller-tube N_{Re} at the upstream temperature and at the wall temperature of the smaller tube,

$$N_{Re} = \frac{[N_{Re}]_{T_{-\infty}} + N_{Re_w}}{2} = \frac{N_{Re_w}}{2}[1+\exp[-\psi(H)]], \quad (6)$$

where

$$\psi(H) = \frac{\Delta H^\dagger}{RT_w}\frac{T_w - T_{-\infty}}{T_{-\infty}} = \frac{\Delta H^\dagger}{RT_w}\left[\frac{1-T'}{T'}\right], \quad (7)$$

$T' = T_{-\infty}/T_w$, T_w is the constant small-tube-wall temperature, and $T_{-\infty}$ is the fluid temperature far upstream from the contraction. The parameter $\psi(H)$ is a measure of the effect of the temperature difference and the dependence of viscosity on temperature. As defined, $\psi(H)$ is positive for heating and negative for cooling.

COMPUTATIONAL PROCEDURES

In order to facilitate the numerical computations, the $r-z$ plane was transformed into the $r-\xi$ plane by a previously used (Carter, 1969; Vrentas et al., 1966) transformation

$$\xi = \tanh kz^* \quad (8)$$

which yielded an upstream axial boundary at $\xi = -1$ and a downstream boundary at $\xi = +1$. The solution space was divided into a square grid, in most cases with ten axial divisions and ten radial divisions in the small tube and, correspondingly, ten axial and ten β radial divisions in the large tube. The following boundary conditions were used:

1. Stream-tube boundary. $\psi^* = 0$, $\partial\psi^*/\partial z^* = 0$, $\omega^* = 0$, $\partial T^*/\partial r^* = 0$.
2. Real-tube-surface boundary. $\psi^* = 0$, $\partial\psi^*/\partial z^* = 0$, $\partial\psi^*/\partial r^* = 0$, $T^* = 1$ parallel to flow, $\partial T^*/\partial z^* = 0$ perpendicular to flow.
3. End conditions. At $z^* = -\infty$, $\omega^* = 0$, $\psi^* = \frac{1}{2}[1 - (r^*/\beta)^2]$ for the stream tube, while $\omega^* = 4r^*/\beta^4$ and $\psi^* = \frac{1}{2} + (r^*/\beta)^2[\frac{1}{2}(r^*/\beta)^2 - 1]$ for the real tube. At $z^* = +\infty$, $\omega^* = 4r^*$ and $\psi^* = \frac{1}{2} + r^{*2}(\frac{1}{2}r^{*2} - 1)$.
4. Tube centerline. $\psi^* = 0.5$, $\partial\psi^*/\partial z^* = 0$, $\omega^* = 0$, $\partial T^*/\partial r^* = 0$.

The differential-difference analogs of Equations (1), (2), and (3), obtained by introducing standard central-difference approximations for the axial derivatives, were solved numerically by combining quasilinearization with the method of lines to yield values of ψ^*, $d\psi^*/dr^*$, ω^*, $d\omega^*/dr^*$, T^*, and dT^*/dr^* at the grid points (see Kelsey, 1971, for complete computational details). We believe that this method yielded greater accuracy in isothermal-flow computations for the same machine time, especially at $N_{Re} \gtrsim 50$, than did the relaxation method previously used (Carter, 1969). However, the relaxation method appeared to be stable at higher N_{Re} in isothermal-flow computations. From the values of $d\psi^*/dr^*$, the values of v_z^* were calculated; and, from the axial differences of ψ^*, the values of v_r^* were calculated. From difference analogs of the original equations of motion, both axial and radial point-pressure gradients were calculated and then integrated to obtain point values of the pressure. Both the axial and the radial pressure gradients were integrated by means of the trapezoidal method. Pressure losses are presented as equivalent lengths L_{eq} defined as the length of the smaller tube in diameters for which the fully-developed-isothermal-flow pressure loss at the tube-wall temperature equals the total excess pressure loss attributable to flow contraction and development in the smaller tube that has accumulated up to axial position z/D.

Results are desirable for ST-RT and RT-RT cases and for a wide range of β, N_{Re}, N_{Pe}, N_{Br}, and $\psi(H)$—a measure of the severity of temperature dependence and the temperature range. However, the number of nonisothermal-flow computations was severely restricted since their cost was relatively high. The computations were restricted largely to ST-RT contracted flow—an approximation of flow into the tubes in the tube sheet of shell-and-tube heat exchangers—and to $\beta = 2$, which approximates the contraction ratio for flow in the tube sheets of many heat exchangers. However, computations can be made at higher values of β; for example, in isothermal Newtonian flow, values of β up to 8 were employed (Christiansen et al., 1972; Kelsey, 1971). The N_{Re} and N_{Pe} ranges were restricted since the computations became unstable at values greater than about 100, depending on the case. A Brinkman number of 0.0 was used in most of the computa-

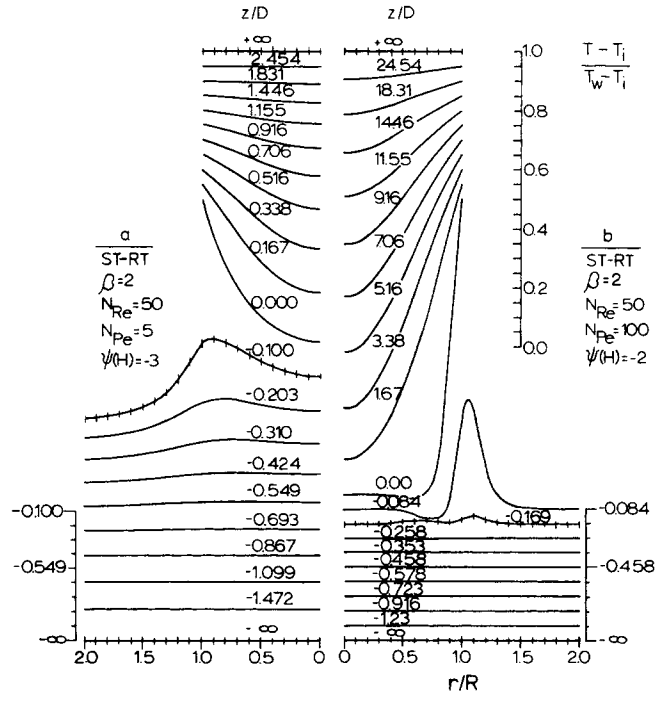

Fig. 1. Typical reduced-temperature profiles (scales adjacent to stream-tube region provide zero references for this region).

tions, which limits most of the computed results to cases in which the effects of temperature increases due to viscous dissipation are negligible; however, some results for temperature-dependent flow with viscous dissipation were obtained (Kelsey, 1971) but will not be discussed here.

NONISOTHERMAL-FLOW RESULTS

Typical temperature profiles are plotted in Figure 1 for two Peclet numbers, $N_{Pe} = 5$ and 100. The N_{Re} indicated is an average Reynolds number for nonisothermal flow, defined by Equation (6). The ratio $(T - T_{-\infty})/(T_w - T_{-\infty})$, where T is a point temperature, is the fraction of the potential temperature change that has been achieved.

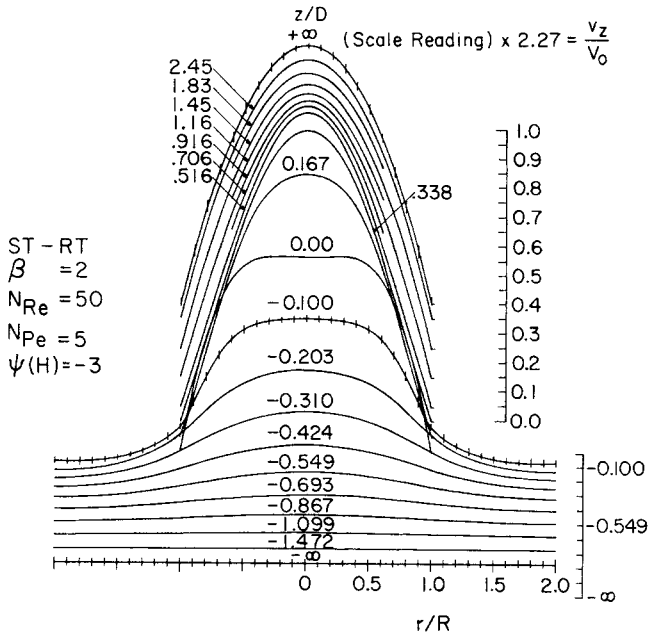

Fig. 2. Typical reduced-axial-velocity profiles (scales adjacent to stream-tube region provide zero references for this region).

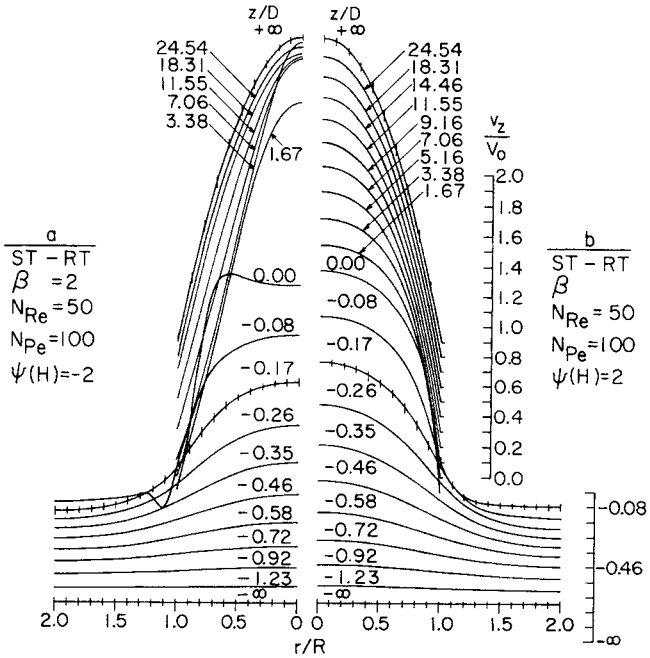

Fig. 3. Typical reduced-axial-velocity profiles (scales adjacent to stream-tube region provide zero references for this region).

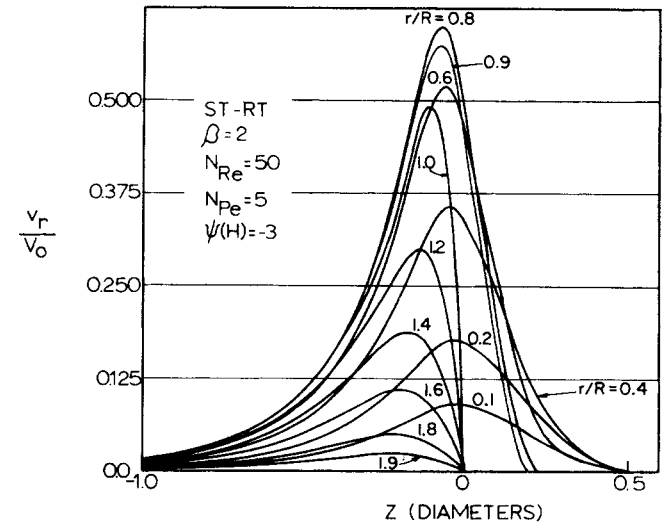

Fig. 4. Typical reduced-radial-velocity profiles.

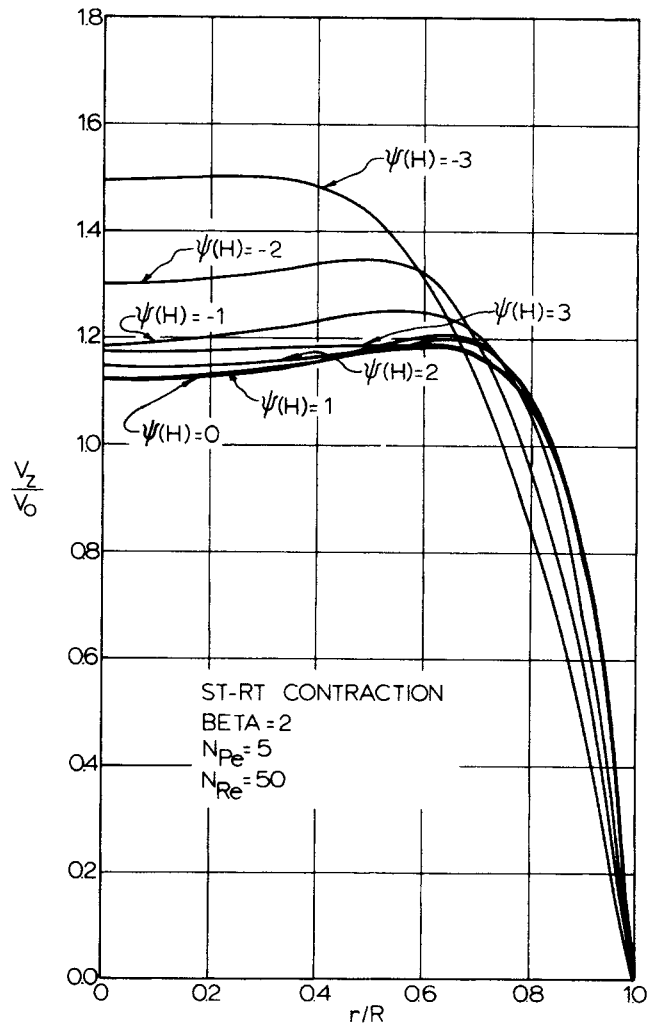

Fig. 5. Reduced axial velocities at the tube entrance ($z = 0$) as functions of the reduced radius and $\psi(H)$ for ST-RT nonisothermal contracted flow.

It will be noted that the temperature profiles begin to deform a significant distance upstream of the heated tube (at $N_{Pe} = 5$, deformation occurs much further than 1½ diameters upstream) in consequence of axial diffusion. Also, at $N_{Pe} = 5$, the potential temperature change has

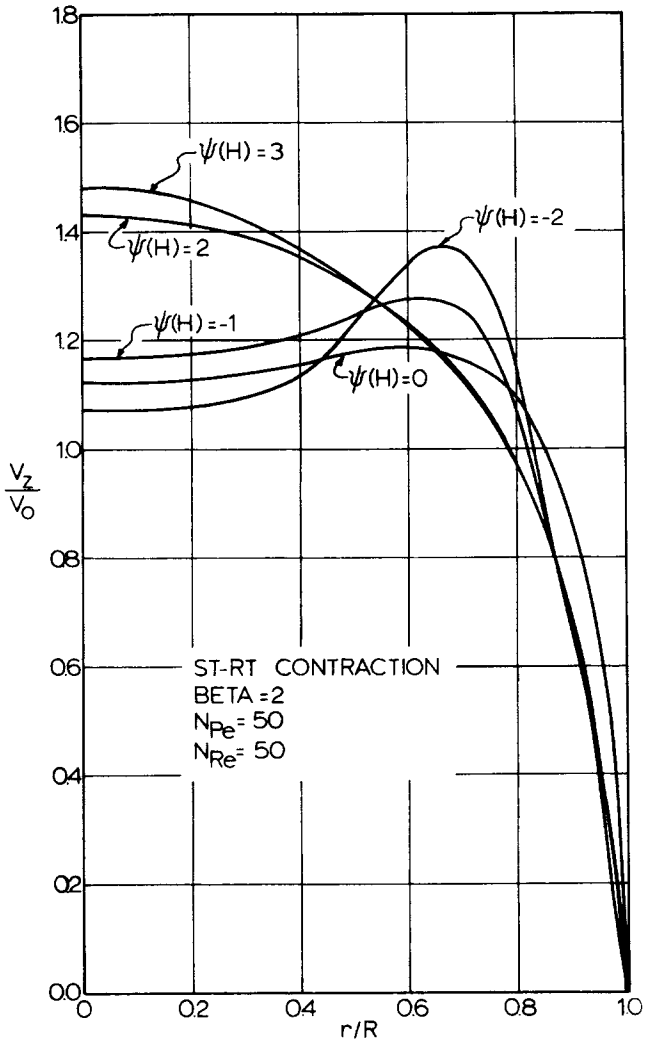

Fig. 6. Reduced axial velocities at the tube entrance ($z = 0$) as functions of the reduced radius and $\psi(H)$ for ST-RT nonisothermal contracted flow.

been accomplished by about 2.5 diam. downstream. At constant N_{Pe} greater than ~50, the computed entrance temperature profiles for varying N_{Re} are approximately superimposable, suggesting that the effect of N_{Re} is small. In Figure 1b, the slight irregularities in the temperature profiles at z/D of 0.00 and −0.084 just outside of r/R of 0.4 are typical for some cases at N_{Pe} of 100 and greater and are believed to be related to computational instabilities. Typical nonisothermal velocity profiles are shown in Figures 2 through 4. As illustrated in Figure 4, radial velocities may be relatively large near the wall at the tube entrance. The radial velocities increase with the extent of cooling, that is, with $-\psi(H)$, and decrease with heating, that is, with $+\psi(H)$.

In Figures 5, 6, and 7, axial-velocity profiles at $z = 0$ are plotted as a function of $\psi(H)$ at N_{Pe} of 5, 50, and 100. Concavities, such as those noted in these three figures, have been observed experimentally (Burke and Berman, 1969) and in previous isothermal-flow computations (Christiansen et al., 1972; Vrentas et al., 1966; Wang and Longwell, 1964) and are discussed by Christiansen et al. (1972). They occur at $N_{Re} > 30$ to 50 in isothermal-flow and cooling cases, are greater in ST-RT contracted flow than in RT-RT contracted flow under comparable conditions, and increase in depth with β and N_{Re}. Also, it will be noted that, with heating, the maximum velocity surrounding the concavity moves closer to the wall, while, with cooling, the opposite occurs.

The effect of N_{Pe} and $\psi(H)$ on L_{eq} is shown in Figures 8, 9, and 10, where L_{eq} is plotted versus z/D, with $\psi(H)$ as a parameter, for N_{Pe} of 5, 50, and 100 at $N_{Re} = 50$. In the cooling cases [$\psi(H)$ is negative], the value of L_{eq} is often less than that for isothermal flow [$\psi(H) = 0$] and, in some cooling cases, is negative in consequence of our use of fully developed flow at the tube-wall temperature as the reference. Of particular interest in Figure 10 is the relatively good agreement between computations using ten and twenty radial divisions at $\psi(H) = 1$.

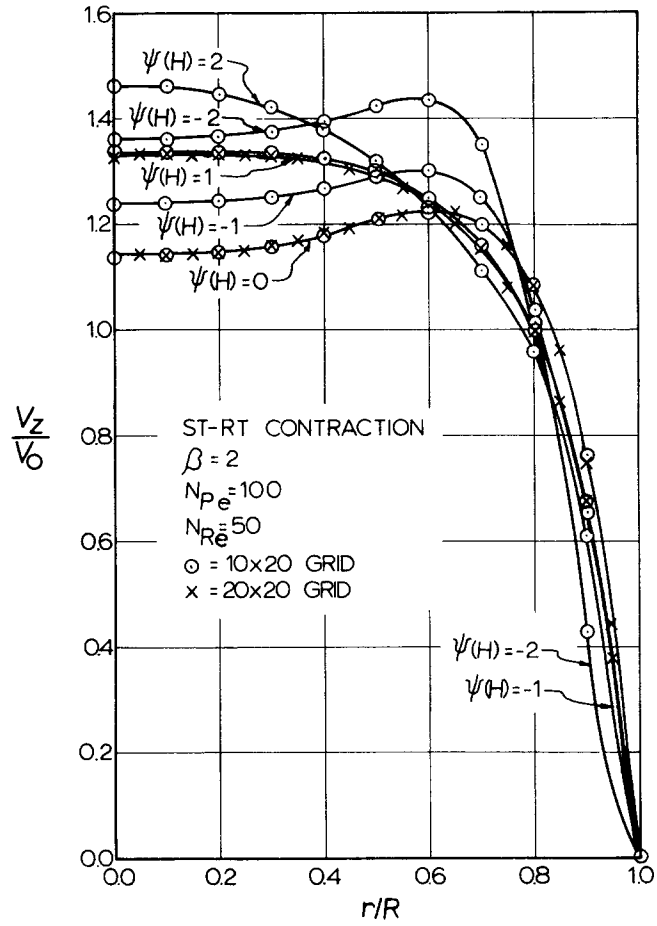

Fig. 7. Reduced axial velocities at the tube entrance ($z = 0$) as functions of the reduced radius and $\psi(H)$ for ST-RT nonisothermal contracted flow.

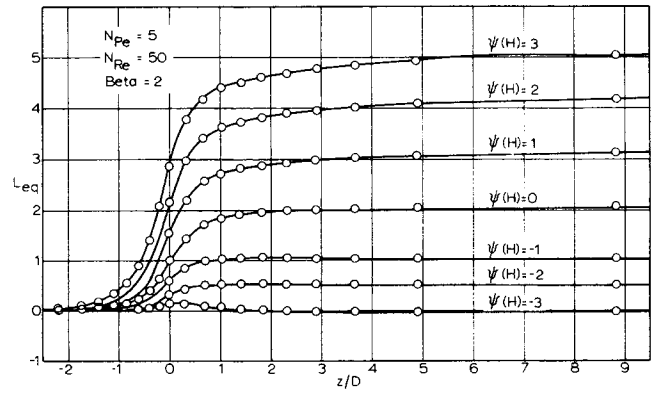

Fig. 8. The equivalent length L_{eq} as a function of the reduced axial length and $\psi(H)$ for ST-RT nonisothermal contracted flow.

As shown in Figure 11 where L_{eq} is plotted versus z/D with N_{Re} as a parameter, L_{eq} increases greatly with N_{Re} at higher N_{Re}. However, based on isothermal-flow computations (Christiansen et al., 1972), data for $N_{Re} = 0.1$ are expected to be essentially the same as those for $N_{Re} = 0.01$; and those for $N_{Re} = 1.0$ would be only slightly higher. Since most nonisothermal-flow computations were made for ST-RT contracted flow at $\beta = 2$, the effect of β and the RT-RT boundary conditions on the results is not certain. However, based on isothermal-flow computations (Christiansen et al., 1972) and preliminary nonisothermal-flow calculations for the RT-RT case (Kelsey, 1971), L_{eq} increases significantly with β up to a value of about 3 for ST-RT contracted flow and up to a value of 6 for RT-RT contracted flow. The ST-RT values of L_{eq} for $\beta = 3$ are less than 5% greater than those for $\beta = 2$. In the case of isothermal flow, values of L_{eq} for RT-RT flow are lower than those for ST-RT flow; for example, the data for RT-RT flow at $\beta = 4$ coincide almost exactly with those for ST-RT flow at $\beta = 3$, and RT-RT data for $\beta = 3$ are only slightly lower than ST-RT data for $\beta = 2$.

In general, the entrance effects extend further upstream with increasing $\psi(H)$ and decreasing N_{Pe}. In the case of $N_{Pe} = 5$ (Figure 8), excess pressures begin to appear as far as 2.5 diameters upstream from the small-tube entrance. Also, it will be observed in Figures 8, 9, and 10 that the entrance length becomes greater with increasing absolute values of $\psi(H)$.

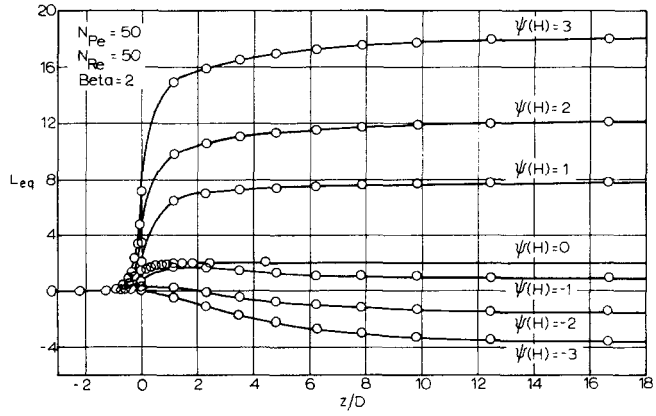

Fig. 9. The equivalent length L_{eq} as a function of the reduced axial length and $\psi(H)$ for ST-RT nonisothermal contracted flow.

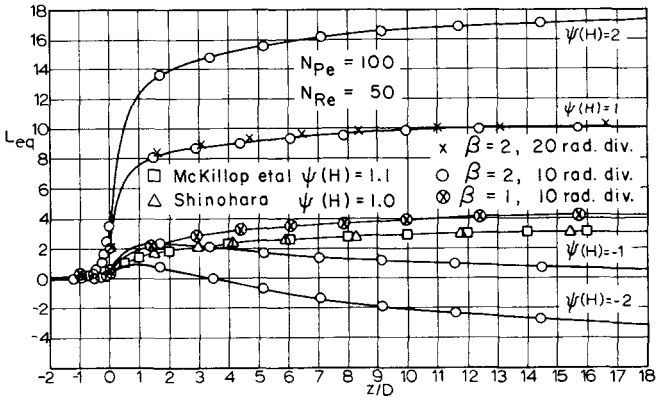

Fig. 10. The equivalent length L_{eq} as a function of the reduced axial length and $\psi(H)$ for ST-RT nonisothermal contracted flow.

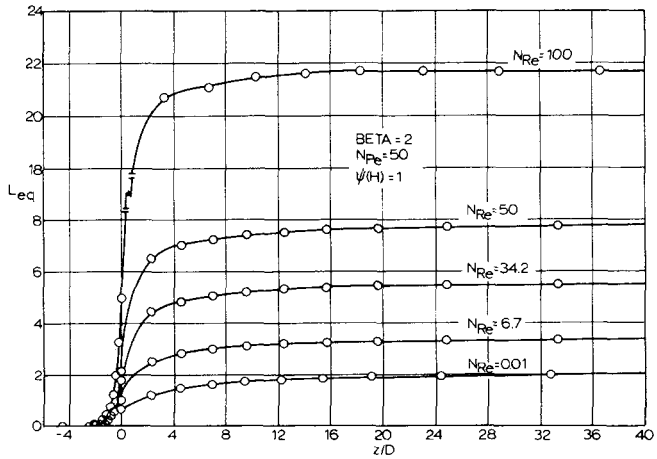

Fig. 11. The equivalent length L_{eq} as a function of the reduced axial length and N_{Re} for ST-RT nonisothermal contracted flow.

DISCUSSION OF RESULTS

The results of several more or less definitive experimental studies for the isothermal, laminar flow of Newtonian and some non-Newtonian fluids through an abrupt contraction from a large real tube into a smaller real tube of circular cross section have been reported (Astarita and Greco, 1968; LaNieve, 1963; Michiyoshi et al., 1966; Ramamurthy, 1970; Ramamurthy and Boger, 1971; Sylvester and Rosen, 1970). However, we are not aware of any experimental studies of ST-RT or RT-RT Newtonian tube-entrance flow accompanied by heat transfer to or from the fluid that are sufficiently definitive for critical evaluation of our computations.

Computed isothermal-flow predictions of L_{eq} at high N_{Re} are less than 3% lower than the experimental results of Sylvester and Rosen (1970) and less than 4% higher than those of LaNieve (1963) but are much lower than the widely varying experimental results at lower N_{Re} (Christiansen et al., 1972). Also, isothermal-flow computations using the present program are almost always within $L_{eq} = 0.1$ of those made with a similar but independent program using the stream-function equations and relaxation (Christiansen et al., 1972).

As shown in Figures 7 and 10, the nonisothermal-flow computations for ten and twenty radial-grid divisions in the flow field are close to each other, indicating that the computations are very nearly converged to a solution.

The solutions of simplified equations of motion and energy for developing but initially flat temperature and velocity fields by Shinohara (1972) in our laboratory and by McKillop et al. (1970) are plotted in Figure 10 for comparison with the presently reported solutions of the more general equations. The results would be expected to be comparable only at $\beta = 1$. The values of L_{eq} from solutions of the simplified equations are lower than those from the general equations, especially for $\beta > 1$, and do not show the existence of an excess pressure loss resulting from axial diffusion upstream of the tube entrance. Velocity and temperature profiles at $\beta = 1$ were far from uniform. For example, at $\beta = 1$, $N_{Re} = 50$, $N_{Pr} = 100$, and $\psi(H) = 1$, the entrance velocity profile is essentially uniform at about 1.2 V_0 out to $r/R \simeq 0.5$; and the entrance temperature profile is uniform at $T_{-\infty}$ out to $r/R \simeq 0.8$. However, the results from solutions of the general equations for $\beta = 1$ and N_{Pr} of the order of unity and greater would be expected to approach those from the simplified equations with the assumption of uniform entrance temperatures and velocities at $N_{Re} \gtrsim 200$, as is the case in

isothermal flow (Christiansen et al., 1972). Unfortunately, we were unable to achieve solutions of the general equations for nonisothermal conditions at $N_{Re} \gtrsim 100$ and/or $N_{Pe} \gtrsim 100$, owing to computational instabilities.

The results are unique in that they represent the first solution of unrestricted equations of motion and energy for temperature-dependent nonisothermal contracted Newtonian flow. The results are believed to be sufficiently accurate for most engineering purposes and should be useful in the design of such equipment as tubular heat exchangers and reactors for conditions within the range of variables included in this study.

ACKNOWLEDGMENT

The authors gratefully acknowledge the financial support of the National Science Foundation, the Advanced Research Projects Agency, and the University of Utah Research Fund.

NOTATION

c_p = heat capacity, cal g^{-1} °K^{-1}
D = tube diameter, cm
f = $-\mu/\rho$, cm^2 sec^{-1}
f^* = $f/(RV_0)$
k = thermal conductivity, cal cm^{-1} sec^{-1} °K^{-1}
k = grid distribution factor in $z - \xi$ plane transformation
L_{eq} = length of smaller tube, in diameters, for which the fully-developed isothermal-flow pressure loss at the tube-wall temperature equals the total excess pressure loss accumulated up to axial point z/D
N_{Br} = Brinkman number
N_{Br_n} = nonshear-rate-dependent Brinkman number
N_{Pe} = Peclet number = $N_{Re}\,N_{Pr} = [\rho\, V_0\, D\, c_p]/k$
N_{Pr} = Prandtl number
N_{Re} = Reynolds number $= \frac{1}{2}[(\rho\, V_0\, D)/\mu]_w\,[1 + \exp[-\psi(H)]]$
r = radial distance, cm
r^* = r/R
R = Boltzman constant per mole, cal mol^{-1} °K^{-1}
R = tube radius, cm
T = absolute temperature, °K
T' = T_{-x}/T_w
T^* = $(T - T_{-x})/(T_w - T_{-x})$
$T_{-\infty}$ = temperature at $z = -\infty$, °K
T_w = tube-wall temperature, °K
v_r = radial velocity, cm sec^{-1}
v_r^* = reduced radial velocity = v_r/V_0
v_z = axial velocity, cm sec^{-1}
v_z^* = reduced axial velocity = v_z/V_0
V_0 = area average velocity, cm sec^{-1}
z = axial distance, cm
z^* = z/R
$-\infty$ = evaluated at $-\infty$
w = evaluated at the wall temperature of the smaller tube

Greek Letters

β = ratio of upstream-tube diameter to downstream-tube diameter
$\dot{\gamma}$ = shear rate, sec^{-1}
$\Delta H^\dagger$ = flow activation energy, cal mol^{-1}
μ = viscosity, g cm^{-1} sec^{-1}
μ_0 = reference viscosity, g cm^{-1} sec^{-1}
ξ = transformed axial distance
ρ = density, g cm^{-3}
τ = shear stress, dynes cm^{-2}
Φ_v = dissipation function, sec^{-2}
Φ_v^* = $(R^2/V_0^2)\Phi_v$
ψ = stream function, cm^3 sec^{-1}
ψ^* = $\psi/(R^2\,V_0)$
$\psi(H)$ = $(\Delta H^\dagger/RT_w)(T_w - T_{-\infty})/T_{-x}$
ω = vorticity, sec^{-1}
ω^* = $R\omega/V_0$
∇^{*2} = $1/R^2[\partial^2/\partial r^{*2} + (1/r^*)(\partial/\partial r^*) + \partial^2/\partial z^{*2}]$

LITERATURE CITED

Astarita, G., and G. Greco, "Excess Pressure Drop in Laminar Flow through Sudden Contraction," *Ind. Eng. Chem. Fundamentals*, **7**, 27 (1968).

Burke, J. P., and N. S. Berman, "Entrance Flow Development in Circular Tubes at Small Axial Distances," Paper presented at the ASME Winter Ann. Meeting, Los Angeles (1969).

Carter, T. R., "Laminar Fluid Flow from a Reservoir up to and through a Tube-entrance Region," Ph.D. thesis, Univ. of Utah, Salt Lake City (1969).

Chen, S. S., L. T. Fan, and C. L. Hwang, "Entrance Region Flow of the Bingham Fluid in a Circular Pipe," *AIChE J.*, **16**, 293 (1970).

Christiansen, E. B., and T. R. Carter, "Non-Newtonian Flow from a Large Tube up to and through the Entrance-flow Region of a Smaller Coaxial Tube of Circular Cross Section," paper presented at the III Congress CHISA, Prague, Czechoslovakia (1969).

Christiansen, E. B., and S. E. Craig, Jr., "Heat Transfer to Pseudoplastic Fluids in Laminar Flow," *AIChE J.*, **8**, 154 (1962).

Christiansen, E. B., and G. E. Jensen, "Laminar Nonisothermal Flow of Fluids in Tubes of Circular Cross Section," *ibid.*, **15**, 504 (1969).

———., "Energy Transfer to Non-Newtonian Fluids in Laminar Flow," pp. 738-747 in *Progress in International Research on Thermodynamic and Transport Properties*, ed. by J. F. Masi and D. H. Tsai, Academic Press, New York (1962).

———., and F. S. Tao, "Laminar Flow Heat Transfer," *AIChE J.*, **12**, 1196 (1966).

Christiansen, E. B., S. J. Kelsey, and T. R. Carter, "Laminar Tube Flow through an Abrupt Contraction," *AIChE J.*, **18**, 372 (1972).

Christiansen, E. B., and H. E. Lemmon, "Entrance Region Flow," *ibid.*, **11**, 995 (1965).

Collins, M., and W. R. Schowalter, "Behavior of Non-Newtonian Fluids in the Entry Region of a Pipe," *ibid.*, **9**, 804 (1963).

Hornbeck, R. W., "Non-Newtonian Laminar Flow in the Inlet of a Pipe," Paper presented at the ASME Winter Ann. Meeting, Chicago (1965).

Jensen, G. E., "Energy and Momentum Transfer to Non-Newtonian Fluids," Ph.D. thesis, Univ. of Utah, Salt Lake City (1963).

Kelsey, S. J., "Isothermal and Nonisothermal, Laminar, Newtonian and Non-Newtonian Entrance-region Flow," Ph.D. thesis, Univ. of Utah, Salt Lake City (1971).

LaNieve, H. L., III, "Entrance Effects in Non-Newtonian Pipe Flow," M.S. thesis, Univ. of Tenn., Knoxville (1963).

Lemmon, H. E., "Fluid Flow in Tubes," Ph.D. thesis, Univ. of Utah, Salt Lake City (1963).

McKillop, A. A., J. C. Harper, H. J. Bader, and A. Y. Korayem, "Variable Viscosity Entrance-Region Flow of Non-Newtonian Liquids," *Intern. J. Heat Mass Transfer*, **13**, 901 (1970).

Michiyoshi, L., K. Mizuno, and Y. Hoshiai, "Studies on the Flow of Slurry through a Pipe, I: Entrance Region of Laminar Flow," *Intern. Chem. Eng.*, **6**, 373 (1966).

Ramamurthy, A. V., Ph.D. thesis, Monash Univ., Melbourne, Australia (1970).

———., and D. V. Boger, "Developing Velocity Profiles on the Downstream Side of a Contraction for Viscous Power-law Fluids," *Trans. Soc. Rheol.*, **15**, 709 (1971).

Rosenberg, D. E., and J. D. Hellums, "Flow Development and Heat Transfer in Variable-viscosity Fluids," *Ind. Eng. Chem. Fundamentals*, 4, 417 (1965).
Shinohara, T., "A Definitive Experimental and Theoretical Study of a Laminar-flow Tubular Reactor," Ph.D. thesis, Univ. of Utah, Salt Lake City (1972).
Sylvester, N. D., and S. L. Rosen, "Laminar Flow in the Entrance Region of a Cylindrical Tube, Part I: Newtonian Fluids," *AIChE J.*, 16, 964 (1970).
Vrentas, J. S., J. L. Duda, and K. G. Bargeron, "Effect of Axial Diffusion of Vorticity on Flow Development in Circular Conduits, Part I: Numerical Solutions," *ibid.*, 12, 837 (1966).
Wang, Y. L., and P. A. Longwell, "Laminar Flow in the Inlet Section of Parallel Plates," *ibid.*, 10, 323 (1964).

Manuscript received August 30, 1971; revision received March 1, 1972; paper accepted March 1, 1972.

Liquid Sorption Equilibria of Selected Binary Hydrocarbon Systems in Type Y Zeolites

On NaY and HY, aromatic compounds are selectively adsorbed in preference to paraffins and naphthenes. Smaller aromatic compounds are adsorbed in preference to larger aromatic compounds. All the compounds studied can be sorbed into the pore structure of the zeolites and the selectivities are primarily a reflection of relative affinity for the zeolite and steric effects rather than a sieving effect.

CHARLES N. SATTERFIELD and CHON S. CHENG

Department of Chemical Engineering
Massachusetts Institute of Technology
Cambridge, Massachusetts 02139

SCOPE

This study arose out of a primary interest in the factors that affect the rates of counterdiffusion of organic liquids in the pores of zeolites, especially the large pore zeolites of interest in catalysis. A knowledge of sorption equilibria is needed to determine the driving force for diffusion as well as being of interest in its own right in separation processes. A knowledge of relative adsorptivities can also be of major value in interpreting catalytic reaction phenomena where two or more species compete for the same type of sites. Single-component and counterdiffusion studies with the same binary systems are described elsewhere (Satterfield and Cheng, 1972 a, b).

CONCLUSIONS AND SIGNIFICANCE

Highly selective adsorption from a binary liquid system can occur on molecular sieve zeolites when both components have full access to the entire fine pore structure. The adsorption is caused by the relative affinity or interaction energy of the molecules for the zeolite structure. On NaY aromatic compounds are selectively adsorbed over paraffins and naphthenes. Within a group of aromatic compounds those having the smallest and most compact structure, for example, benzene and cumene, are selectively adsorbed over larger aromatics, for example, 1,3,5-triisopropyl benzene. On at least one system (trans-decalin —*n*-decane) the separation factor is little affected by temperature.

More limited studies on HY indicate that the separation factor between aromatic molecules, paraffins, and naphthenes is less than on NaY, which is consistent with the lower interaction energy between HY and aromatics.

Selective adsorption effects of the type studied here can lead to marked selectivity phenomena in the catalytic reaction of multicomponent systems.

Correspondence concerning this paper should be directed to C. N. Satterfield. C. S. Cheng is with Mobil Chemical Company, Research and Development Laboratories, P. O. Box 240, Edison, New Jersey 08817.